Picosecond real time study of the bimolecular reaction O (3 P)+ C 2 H 4 and the unimolecular photodissociation of CH 3 CHO and H 2 CO

Osama K. Abou-Zied and J. Douglas McDonald

Citation: The Journal of Chemical Physics **109**, 1293 (1998); doi: 10.1063/1.476679
View online: http://dx.doi.org/10.1063/1.476679
View Table of Contents: http://scitation.aip.org/content/aip/journal/jcp/109/4?ver=pdfcov
Published by the AIP Publishing

Picosecond real time study of the bimolecular reaction $O(^3P)+C_2H_4$ and the unimolecular photodissociation of CH_3CHO and H_2CO

Osama K. Abou-Zied[a] and J. Douglas McDonald[b]
Department of Chemistry, University of Illinois, Urbana–Champaign, Urbana, Illinois 61801

(Received 15 December 1997; accepted 14 April 1998)

The bimolecular reaction of $O(^3P)$ with ethylene and the unimolecular photodissociation of acetaldehyde and formaldehyde have been studied using a picosecond pump/probe technique. The bimolecular reaction was initiated in a van der Waals dimer precursor, $C_2H_4 \cdot NO_2$, and the evolution of the vinoxy radical product monitored by laser-induced fluorescence. The NO_2 constituent of the complex was photodissociated at 266 nm. The triplet oxygen atom then attacks a carbon atom of C_2H_4 to form a triplet diradical (CH_2CH_2O) which subsequently dissociates to vinoxy (CH_2CHO) and H. The rise time of vinoxy radical production was measured to be 217 $(+75-25)$ ps. RRKM theory was applied and a late high exit barrier was invoked in order to fit the measured rise time. The structure and binding energy of the van der Waals complex have been modeled using Lennard-Jones type potentials and the results were compared with other systems. The unimolecular side of the potential energy surfaces of this reaction has been investigated by photodissociating acetaldehyde at the same pump energy of 266 nm. The resulting photoproducts, acetyl radical (CH_3CO) and formyl radical (HCO), have been monitored by resonance enhanced multiphoton ionization (REMPI) combined with a time-of-flight mass spectrometer. The similarity in the measured evolution times of both radicals indicates the same photodissociation pathway of the parent molecule. The photodissociation rate of acetaldehyde is estimated from RRKM theory to be very fast $(3\times10^{12}\ s^{-1})$. The $T_1 \leftarrow S_1$ intersystem crossing (ISC) rate is found to be the rate determining step to photodissociation and increases with energy. The REMPI mechanism for the production of CH_3CO^+ is proposed to be the same as that of $HCO^+(2+1)$. The HCO product from the photodissociation of formaldehyde at 266 nm reveals a faster $T_1 \leftarrow S_1$ ISC rate than in acetaldehyde. © *1998 American Institute of Physics.* [S0021-9606(98)00528-5]

I. INTRODUCTION

Several radicals are found to play important roles in combustion processes[1,2] and atmospheric reactions.[3] Among these radicals, which are the focus of this paper, are formyl (HCO), acetyl (CH_3CO), and vinoxy (CH_2CHO). For spectroscopic studies, these and other radicals are usually obtained by unimolecular photodissociation of small organic compounds such as formaldehyde, acetaldehyde, and ethyl or methyl vinyl ether. Important examples in combustion processes and in atmospheric chemistry are the reactions of oxygen atoms with a number of unsaturated hydrocarbon species.

Reactions of both singlet and triplet oxygen atoms are common. The reaction of triplet oxygen with ethylene has been studied by molecular beam scattering[4] and by laser fluorescence,[5–8] as well as by infrared chemiluminescence.[9] Consider the Born–Oppenheimer potential energy surfaces[4,7,10,11] shown in Fig. 1 (adapted from Refs. 7 and 10). Basically, there are three channels observed for the reaction of $O(^3P)$ with ethylene,

$$O(^3P)+C_2H_4 \rightarrow CH_2CHO+H, \quad \Delta H=-17 \text{ kcal/mol} \quad (1)$$

$$\rightarrow CH_3+HCO, \quad \Delta H=-28 \text{ kcal/mol} \quad (2)$$

$$\rightarrow CH_2CO+H_2, \quad \Delta H=-82 \text{ kcal/mol.} \quad (3)$$

Channels (2) and (3) which produce formyl radical and ketene occur on the ground singlet surface produced by (triplet→singlet) intersystem crossing (ISC) at the CH_2CH_2O diradical and could be quite slower.[4] The first channel produces a vinoxy radical which can be reached in two ways: one directly through $^3TS_0$, the triplet state of CH_2CH_2O, and $^3TS_1$; the other by ISC to singlet CH_2CH_2O, across $^1TS_1$ to acetaldehyde, across $^1TS_2$ to vinyl alcohol, and then uphill to vinoxy+H. The latter is exceedingly improbable at energies just above threshold (−10 kcal/mol in Fig. 1) because several products can be reached directly from S_0 acetaldehyde by lower energy processes. The former is the only reaction channel that comes directly from triplet CH_2CH_2O, and it competes only with ISC. So most vinoxy will come from the direct channel. The part of the potential surface to the right of the diradical in Fig. 1 can be easily studied by unimolecular photodissociation of acetaldehyde.

The above $O+C_2H_4$ reaction has already been studied by laser-induced fluorescence (LIF) starting from a van der Waals complex of ethylene with NO_2. It is found from LIF that the vinoxy product from the van der Waals complex with a 355 nm pump is cold,[7] as is that found in a crossed beam LIF study at the same energy.[5] At 266 nm pump in the

[a]Present address: Department of Chemistry, California Institute of Technology, Pasadena, California 91125.
[b]Author to whom correspondence should be addressed.

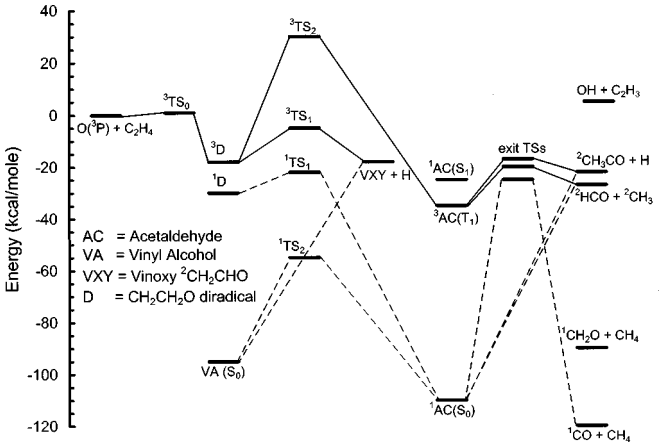

FIG. 1. Energy levels of the reaction of $O(^3P)+C_2H_4$ and of the acetaldehyde photodissociation. Energies are in correct order but not precisely placed. Solid lines representing reaction coordinates represent triplets, dashed ones represent singlets. (Taken from Refs. 7 and 10.)

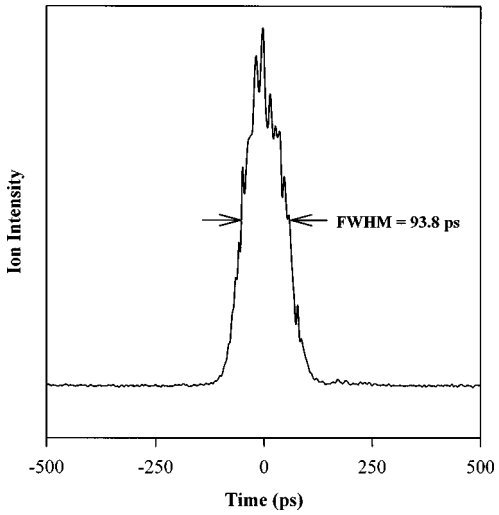

FIG. 2. A characteristic cross correlation of the output from the pump beam at $\lambda_{pump}=532$ nm and the probe beam from one of the continuum amplifier chains at $\lambda_{probe}=692$ nm.

beam, Loison *et al.*[7] find vinoxy to still be colder than the statistical limit. At a translational energy of 8 kcal/mol Schmoltner *et al.*[4] found a broad distribution of product translational energies, with a very large amount of product near the high velocity energetic limit. In bulk, Loison *et al.*[8] indicate hot vinoxy by LIF, but their experiment is so strongly collisional that it really has no bearing on the single collision experiment. However, Loison *et al.* find no evidence of a HCO radical from the complex at a time delay between pump and probe of 20 ns. At longer times they see a HCO radical, but indicate that this is under collision conditions. Schmoltner *et al.* reported the ratio of the relative cross sections for the production of HCO and CH_2CHO to be 2.5 ± 0.9 in their crossed molecular beam experiment under the assumption that there is no contribution from other reaction channels.

In this paper, we further investigate the above complex system under cold isolated conditions in a pump–probe experiment. We report our picosecond observation of the time evolution of the vinoxy radical produced from the van der Waals complex of ethylene with NO_2. NO_2 is used as a precursor of atomic oxygen since photodissociation of NO_2 has been well studied[12,13] and it is known that it dissociates at $400>\lambda>244$ nm to produce a high yield of $O(^3P)$. The geometry of the complex is calculated using a Lennard-Jones 6–12 atom–atom potential which shows that the O atom attacks the ethylene molecule at one end. We also extend our investigation of this chemical system to the unimolecular photodissociation of acetaldehyde. This photodissociation can be studied by probing both HCO and CH_3CO radicals as the products. We compare the time evolution of HCO produced from acetaldehyde to that from the photodissociation of formaldehyde at the same photolysis energy. The Rice–Ramsperger–Kassel–Marcus (RRKM) theory is applied here in order to estimate the reaction barriers to dissociation.

II. EXPERIMENT

The laser system used in this study provides two picosecond pulses which are continuously tunable over a broad spectrum. The details of the experimental apparatus and techniques employed have been described in detail elsewhere.[14,15] Briefly, a cw mode-locked dye laser generates near picosecond laser pulses (0.2 nJ 563–700 pulses 0.6 ps long) by pumping it with a pulse-compressed (6 ps long compressed part) Nd:YAG laser. Residual 1.064 μm pulses from the cw Nd:YAG laser drive a multistage amplifier which produces about 10 mJ each at 532 and 355 nm at a repetition rate of 12 Hz.

A three-stage amplifier chain generates 50–150 μJ of 563 nm light which is used for supercontinuum generation, for producing other wavelengths, 363–900 nm. A tunable, bandwidth-selectable, nontime dispersive monochromator selects the probe wavelength from the continuum. This is amplified to about 80 μJ in a three-stage dye amplifier chain.

In one experiment, Exalite 398 or DPS dyes were used to produce 395–425 nm light, which was used directly. The output of this channel was 60–90 μJ. In another experiment, light at 640–710 nm amplified in LDS 698 or DCM was then doubled to produce 5–8 μJ pulses at 320–360 nm. In all experiments, the pump light was provided by 15 μJ of quadrupled YAG laser output at 266 nm. This light was sent a constant distance to the interaction region which was then used to dissociate NO_2, acetaldehyde, and formaldehyde. The probe light was variably delayed prior to entering the interaction region. A typical cross correlation of the pump and probe is presented in Fig. 2. The zero time for the experiment was established by overlapping the two beams externally using a pinhole and then carrying out a pump/probe type experiment.

The molecular beam apparatus was changed in order to suit two different kinds of experimental detection, resonance enhanced multiphoton ionization (REMPI) and LIF. For REMPI, experiments were conducted in a doubly skimmed, double-differentially pumped three-chamber vacuum system. The initial chemical expansion occurs there through a specially designed corrosion-resistant pulsed solenoid valve with a 0.76 mm orifice.[16] REMPI products are produced in

the source of a Wiley–McLaren time-of-flight mass spectrometer (TOFMS) with a flight path of 1 m. The ultimate mass resolution of this spectrometer is 1:110 amu. The two laser beams enter at the base of the TOFMS, mutually orthogonal to the detection axis and the molecular beam and are tightly focused and crossed exactly in the region of interaction. Ions are detected with a cascade pair of leaded glass microchannel plate electron multipliers. Transient data from the TOFMS are handled with a 2048 channel transient digitizer (Biomation model 8100). The transient recorder collects a complete mass spectrum from the TOFMS with each laser or electron pulse, allowing many mass peaks to be monitored simultaneously. Data acquisition and experimental control are handled by a personal computer. Electron-impact methods are also employed for monitoring beam conditions.

For LIF experiments, only a single vacuum chamber is used. A pulsed, unskimmed General Valve pulsed valve (Part 9-181-900) is used as the beam source. Typical operating conditions were obtained with a nozzle diameter of 0.4 mm and exciting 5–10 mm downstream from the nozzle ($x/D=10-25$) in order to optimize the signal. The pulsed valve is operated at 12 Hz (for both REMPI and LIF), based on the capacity of the vacuum pumps. The LIF signal is focused and detected by an RCA 7265 photomultiplier tube. The two laser beams enter the main chamber and exit it through four pairs of homemade black rings which act as baffles placed inside the chamber in order to reduce the amount of scattered laser light. The two laser beams are unfocused in order to illuminate a large area of the sample (about 2–3 mm in diameter).

Ultrahigh purity NO_2 (Air Products and Chemicals, Inc.) and C_2H_4 (99.999%, MG Industries) were used as received and premixed before expansion in a separate light-shielded container to obtain a mixture of about 1%–2% NO_2 and 2%–5% C_2H_4 in 20–30 psig He (ultrahigh purity, Matheson). No reaction was observed between NO_2 and C_2H_4 in the dark for long time mixing. Cutoff filters were used in order to avoid scattered laser light and to block any detection of NO_2 emission produced by excitation of N_2O_4.[17] This emission was strongly detected when only NO_2 was expanded without ethylene, as observed by Loison *et al.*[6] Fluorescence from vinoxy was detected in the wavelength range (360–440) nm which hosts most of its emission transitions following excitation to its 0_0^0 band origin.[18] Our short time delay between the laser pulses made dissociation of NO_2 at 355 nm impossible due to interference by the excitation laser scattering.

Acetaldehyde (99%, Aldrich Chemical Company, Inc.) was used after distillation and was cooled down to $-40\,^{\circ}C$ in a mixture of dry ice in 1:1 *o*-(97%) and *m*-(99%) xylenes (Aldrich Chemical Company, Inc.) and then allowed to flow slowly by bubbling about 5 psig of He through it prior to expansion. This procedure greatly minimized the dimer formation of acetaldehyde to essentially zero as can be seen in our mass spectra.

Formaldehyde monomers were obtained by mixing about 3 g of paraformaldehyde (95%, Aldrich Chemical Company, Inc.) and 3 g of anhydrous $MgSO_4$ (Fisher Scientific) in a plastic tube connected to the valve and containing wadded cotton wool prior to the nozzle in order to filter out particulates. The tube and the nozzle were heated to about 70 °C causing the paraformaldehyde to liberate formaldehyde monomers and water. The latter was trapped by the $MgSO_4$. Formaldehyde vapor was then expanded into the nozzle in 5 psig He.

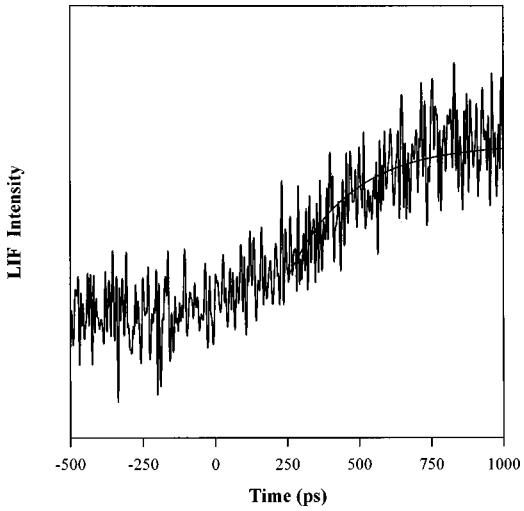

FIG. 3. Photoinitiated reaction starting from $C_2H_4 \cdot NO_2$ precursor. The transient signal is the fluorescence of CH_2CHO probed at 347.2 nm. The rise time is estimated as 217 ± 38 ps according to a single-exponential fit.

III. RESULTS

The time evolution of fluorescence from the vinoxy radical produced from a $C_2H_4 \cdot NO_2$ van der Waals complex is shown in Fig. 3. In this experiment, pump light at 266 nm is used to dissociate NO_2 into NO and $O(^3P)$. $O(^3P)$ subsequently interacts with C_2H_4 in the restricted geometry complex to yield the vinoxy radical [reaction (1)]. The radical is detected by tuning the probe pulse to its 0_0^0 $[B(^2A'') \leftarrow X(^2A'')]$ transition at 347.2 nm[19] and observing its LIF evolution as a function of the time delay between the pump and the probe pulses.

Attempts were made to detect the REMPI of the vinoxy radical by probing at the frequency of its 0_0^0 band through $1+2$ REMPI, or probing its $1+1$ REMPI in the blue tail of its absorption spectrum. All these attempts failed and we attribute this to the very small signal-to-noise ratio (S/N). The mass spectra resulting from these attempts did not show any evidence of van der Waals formation or vinoxy. We should mention here that the area illuminated by the two crossed laser beams in the REMPI experiment is much smaller than that in the LIF experiment as discussed in Sec. II. This will greatly lower the possibility of targeting some of the complexes formed in the beam. We carried out an electron impact ionization experiment in order to detect how much complex is formed. The mass spectrum of this experiment is shown in Fig. 4, which shows the amount of the complex between ethylene and NO_2 to be no more than about $\sim 1\%$ of the NO_2 mass peak. It is difficult to measure from such ionization spectra the exact distribution of clusters in a beam,[20] but it is not difficult to ensure that the smallest cluster, i.e., the dimer, is dominant. We did that by looking at

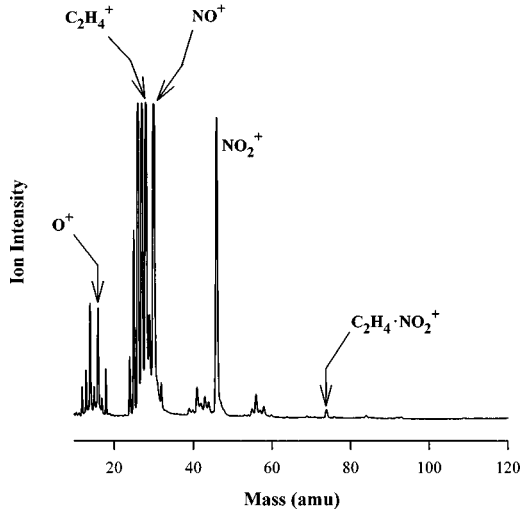

FIG. 4. An electron impact spectrum used to characterize the molecular beam of C_2H_4 and NO_2 in the interaction region. Most unmarked small peaks are residual background.

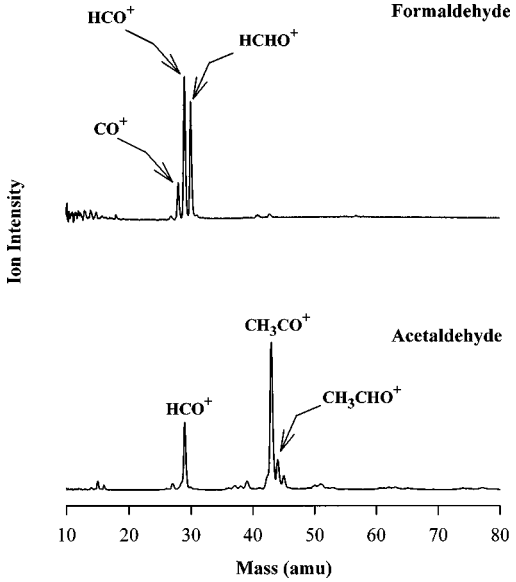

FIG. 5. Mass-selected ion yield spectra of the photodissociation of formaldehyde (upper) and acetaldehyde (lower). The wavelengths used are $\lambda_{pump} = 266$ nm and $\lambda_{probe} = 400$ nm.

higher cluster masses in our $C_2H_4+NO_2$ beam and have found that, at the concentrations employed in our experiment, the higher cluster ion concentration drops off by an order of magnitude for every added molecule.

The transient shown in Fig. 3 is the sum of several scans in order to enhance S/N. This time evolution is fitted to a single exponential rise time of 217 ± 38 ps (statistical uncertainty only), using a nonlinear least-squares fitting routine. We did not fit the whole range starting from the zero of timing because of the large slow rise resulting from the overlapping of the two laser beams in time within the region 0–250 ps (see Fig. 2). It is our opinion that such fitting is not a valid procedure since even slight pump laser saturation can change the shape of the signal in this region. Changing the start point from 250 ps changes the fit rise time more than ± 38 ps. A good guess at possible systematic errors is -50 $+75$ ps.

Acetaldehyde and formaldehyde were both dissociated by the 266 nm pump light. The probe wavelength was tuned to the REMPI of HCO at about 400 nm by two-photon excitation to mostly the $3p\ ^2\Pi$ state, followed by ionization by absorption of one more photon $(2+1)$.[21] We measured the REMPI-TOFM spectra shown in Fig. 5. It is clear that both acetaldehyde and formaldehyde dissociate cleanly at 266 nm. As shown in Fig. 5, we also detected other fragments such as CO^+ (from formaldehyde) and CH_3CO^+ (from acetaldehyde) at the same probe wavelength. Several very weak peaks were observed in our mass spectra similar to some of these observed by Fisanick *et al.*[22] and Shin *et al.*,[23] which are assigned to several fragments from the parent acetaldehyde. By shining only the pump light we still see some fragments which indicates multiphoton absorption processes at the pump wavelength. Multiphoton ionization (MPI) was detected by exciting acetaldehyde to its $3s \leftarrow n$ Rydberg state in the wavelength range 363–354 nm.[22,23] We could minimize the signals due to the pump only by lowering the pump laser power, but could not avoid them completely. This problem does not affect time-dependence scans since the signals due to the pump light are considered as a constant background throughout the time scan. The observed intensity of the CH_3CO^+ peak at $m/z = 43$ is twice that of HCO^+ $(m/z = 29)$ in the mass spectrum of acetaldehyde. This observation is in contrast to the previous work[22,23] in which the mass peak of HCO^+ was found to be the most intense peak.

We measured evolution times for both HCO and CH_3CO at the same probe wavelength of 400 nm as products from the photodissociation of acetaldehyde. The time evolution of HCO and CH_3CO are shown in Fig. 6. Both scans exhibit single-exponential rise times of 622 ± 34 and 667 ± 43 ps, respectively (with a systematic error of $+100$–50 ps). Changing the probe wavelength to a region away from the

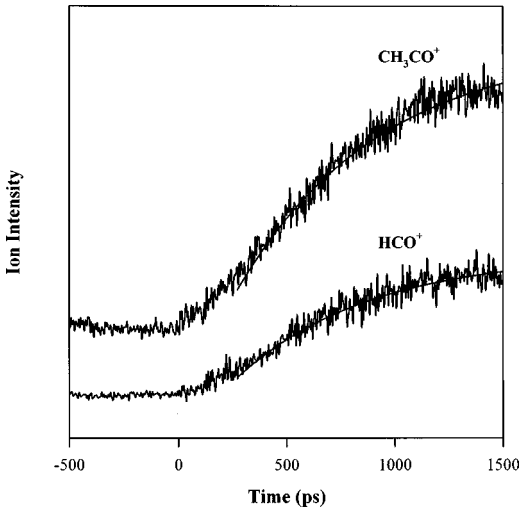

FIG. 6. Transient signals for HCO^+ and CH_3CO^+ produced from the photodissociation of acetaldehyde at $\lambda_{pump} = 266$ nm and probed at $\lambda_{probe} = 400$ nm. The REMPI intensity is recorded as a function of the pump–probe delay. The rise times are estimated as 662 ± 34 ps for HCO^+ and 667 ± 43 ps for CH_3CO^+ according to single-exponential fits.

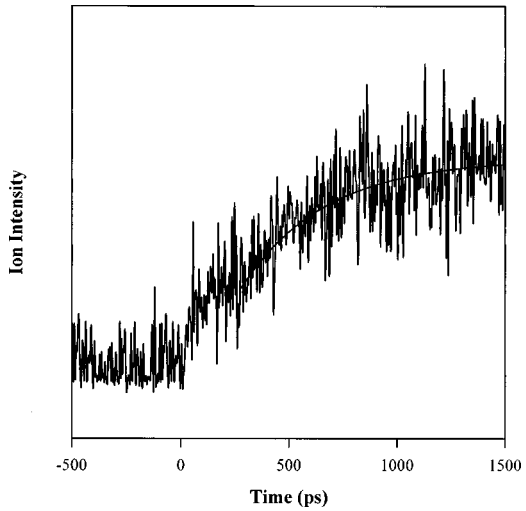

FIG. 7. Transient signal for HCO^+ produced from the photodissociation of formaldehyde at $\lambda_{pump}=266$ nm and probed at $\lambda_{probe}=400$ nm. The REMPI intensity is recorded as a function of the pump–probe delay. The rise time is estimated as 390 ± 64 ps according to a single-exponential fit.

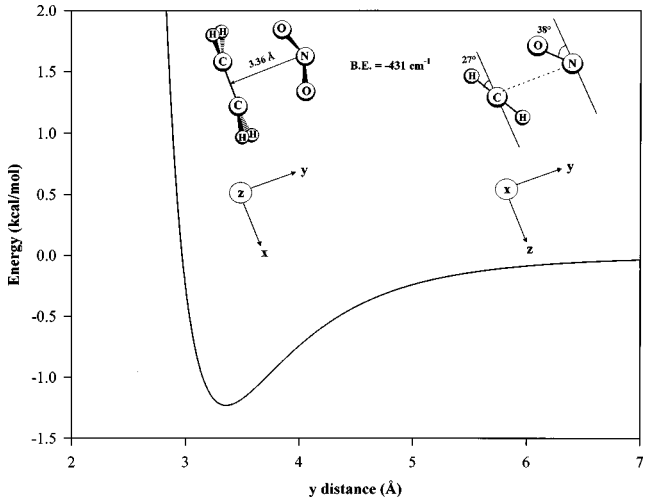

FIG. 8. One-dimensional potential energy surface for the $C_2H_4\cdot NO_2$ complex calculated using the sum of Lennard-Jones atom–atom potentials as a function of the y distance between both adducts. The coordinate system is shown and has its origin at the nitrogen atom. The equilibrium geometry of the complex is also shown in two views.

$(2+1)$ resonant transition of the fragments causes a step at time equal to 0 between the two lasers whose rise time is contained in the first 250 ps, which are disregarded in our fits. This step is due to a $(1+1+1)$ REMPI resonant transition in acetaldehyde.

The formation of the acetyl radical (which is isomeric to vinoxy radical) from acetaldehyde was verified by tuning the probe to the 0_0^0 transition of vinoxy radical at 347.2 nm and measuring its LIF (similar to ethylene and NO_2 experiment). We did not observe any vinoxy fluorescence at this wavelength, which indicates that the vinoxy radical is not one of the products in the acetaldehyde photodissociation.

Finally, the evolution of HCO produced from the dissociation of formaldehyde is shown in Fig. 7. A single-exponential rise time of 390 ± 64 ps was obtained for HCO, again with a larger possible systematic error of $+150-100$ ps.

IV. DISCUSSION

A. Reaction of O(^3P) with C_2H_4

The interaction between C_2H_4 and NO_2 is initiated from the precursor dimer, $C_2H_4\cdot NO_2$. This van der Waals complex is nonreactive and contains the reactants in a restricted geometry, which determines the initial conditions of the reaction upon photodissociation. For example, by orienting the two molecules in the complex relative to each other, the dimer structure determines the initial separation of NO_2 from C_2H_4 and the resultant recoil direction of the particles upon photodissociation. The equilibrium geometry of the complex is not known experimentally, through high resolution spectroscopy, although it is reasonably well known for homologous systems such as $C_2H_4\cdot SO_2$ and $C_2H_4\cdot O_3$.[24,25]

We have calculated the geometry of $C_2H_4\cdot NO_2$ by using Lennard-Jones (LJ) 6-12 atom–atom potential functions.[26] In these calculations, the geometries of both C_2H_4 and NO_2 are given by their ground state equilibrium molecular structures determined by spectroscopic methods.[27] These geometries are considered to be retained in the complex. The binding energy is calculated as a function of the position of NO_2 with respect to C_2H_4. The binding energy is calculated at each geometry by a pairwise summation of attractive and repulsive atom–atom potentials. Accordingly, the ground state binding energy, $E(R)$, is given by[26]

$$E(R)=\sum_i \sum_j \left(-\frac{A_{ij}}{R_{ij}^6}+\frac{B_{ij}}{R_{ij}^{12}}\right), \tag{4}$$

where A_{ij} and B_{ij} are empirically determined attractive and repulsive terms, respectively, for the interactions between atoms i (in C_2H_4) and j (in NO_2) and their values are calculated from the parameters given by Nemethy *et al.*[26] R_{ij} is the distance between atoms i and j. Electrostatic effects are large for the similar molecule $C_2H_4\cdot SO_2$. Using only electrostatic attractive terms, Andrews *et al.*[24] calculated a variation from minimum to maximum of about 800 cm^{-1} in their figure corresponding to our Fig. 8. However, for $C_2H_4\cdot NO_2$, these effects are only 18% (160 cm^{-1}) as great due to the smaller dipole moment of NO_2 and the most stable geometry is predicted to be exactly the same as for the pure LJ calculations. Hence all simple calculations and experiments on similar systems predict the same geometry for $C_2H_4\cdot NO_2$.[24,25]

The results of these calculations show that the most stable conformation has a plane of symmetry which bisects the O–N–O angle and the C═C bond of ethylene. This geometry places the N atom closest to the C═C bond, whereas each oxygen atom is closest to one carbon atom of ethylene. Figure 8 displays this geometry and shows how the potential energy curve changes with the distance between the N atom and the center of the C═C bond in a Morse-type potential. The equilibrium geometry places the NO_2 molecule with a tilt angle of 38° with respect to the xz plane (the coordinate system is shown in Fig. 8). The ethylene molecule is also tilted with respect to the same plane by 27°. The tilt of both

molecules affects only the positions of the oxygen atoms of NO_2 and the hydrogen atoms of C_2H_4. The resulting overall symmetry of the complex is C_s. The binding energy of the most stable conformation is calculated to be $-431\ cm^{-1}$ (perhaps $-500\ cm^{-1}$ including the dipole–quadrupole term) and the equilibrium distance between the N atom and the center of the C═C bond is 3.36 Å. The distance between the O atom and the C atom is calculated to be 2.73 Å.

Ab initio calculations on a similar system ($C_2H_4 \cdot O_3$), show that in order for the complex to reach the transition state the distance between the oxygen and the carbon atoms should be $\sim 2.0-2.3$ Å,[25] or 1.88 Å.[10] We have used the above potentials with an estimated electrostatic term to study rotation of the NO_2 molecule with respect to the C_2H_4 moiety. The barrier to the rotation of the oxygen atom directly toward ethylene (rotation around the x axis) to form a C_{2v} symmetry is only about $100\ cm^{-1}$. The barrier to placing one oxygen atom directly above the C═C bond, with the nitrogen atom also directly above it (rotation around the z axis), is much larger, greater than $200\ cm^{-1}$.

The calculated equilibrium geometry for the complex may not lead directly to the transition state if the oxygen atom leaves NO after dissociation with a zero impact parameter, however three factors should be considered: first, there are large amplitude zero-point quantum fluctuations in the geometry of the complex. Second, the average exit channel impact parameter for oxygen leaving NO is about 1 Å at our pump energy.[28] Third, excitation at 266 nm leaves NO_2 highly vibrationally excited before dissociation. Based on the results on similar systems,[10,25] the oxygen atom has to travel only about 1 Å toward the carbon atom of ethylene in order to reach the transition state. These three factors are expected to place the oxygen atom in the exact direction which will eventually lead to the reaction for a substantial fraction of NO_2 dissociations. Although NO may need to travel away from the interaction region in order to be completely inactive to the diradical intermediate, the left over NO fragment in the vicinity of the diradical is not expected to affect it through what is known as the ''three body effect'' or ''trapped atom effect.'' In comparison with other systems, a study was conducted on the $HI \cdot CO_2$ system,[29,30] in which the very heavy I atom is ''left over'' in the vicinity of the actual reaction, and sees no overt effects of its presence on the reaction. However, dissociation of ozone is apparently severely perturbed by complexation even with the normally rather inert water molecule,[31] so that the leaving oxygen may be in a different electronic state. We do not expect this problem to afflict our system, since neither NO nor O has a different electronic state accessible at our pump energy, other than low energy spin–orbit states.

After dissociation of NO_2, the formation of the vinoxy radical from the reaction of O with C_2H_4 takes place by electrophilic addition of the oxygen atom in its ^3P state to one of the carbon atoms of ethylene. Cvetanovic[32,33] and Schmoltner *et al.*[4] have suggested that, in the absence of stabilizing collisions, this first step leads to the formation of the triplet diradical CH_2CH_2O (^3D in Fig. 1), followed by fragmentation to hydrogen atom and vinoxy radical. Buss *et al.*[34] and Schmoltner *et al.*[4] confirm, through their molecular beam experiment, that the formation of vinoxy is a major product in this bimolecular reaction from the measurements of product angular distributions (obtained by extrapolation from lower energies) but not (at their energy) the most common product. In our beam experiment, dissociation of NO_2 at 266 nm leaves an average of 18 kcal of energy available as translation of O relative to NO, in a very broad distribution.[35] Relative to the ethylene, this becomes 7.5 kcal/mol. This is slightly higher than what Schmoltner *et al.* used.[4] Schmoltner *et al.* also indicate that the vinoxy angular distribution could suggest a lifetime of the triplet diradical of about one rotational period at about 6 kcal incoming translational energy. However, their data appear to us to indicate that the lifetime at the average J value would be at least 4 times the rotational period (3 ps) or 12 ps.[36] Our measured rise time of vinoxy (of 217 ps at an even higher energy) does not agree with this argument and we believe that, given the difficulties of their experiment, their distribution is within their systematic errors of being actually flat.

The formation of vinoxy radical takes place via the $^3TS_1$ transition state[5] (see Fig. 1). We calculated the rate of dissociation of the diradical to vinoxy and H by RRKM theory. The vibrational frequencies for the diradical intermediate used in our calculations were taken from the *ab initio* calculated values by Dupuis *et al.*[37] (reduced 10%). Using the energies calculated by Fueno *et al.*[10] for the diradical intermediate (^3D), and for the exit channel ($^3TS_1$), the calculated rate is 31.7 ps, which is about sevenfold faster than our measured value. Given the nature of their calculations of the energy barriers (based on inadequate basis sets or inadequate configurations) their calculated values must be considered approximate ± 5 kcal/mol or even worse. In order to reproduce our measured rise time of vinoxy, the $^3TS_1$ transition state must be placed as a late high barrier at about 2.5 kcal/mol above the 0 energy in Fig. 1, which is 4 kcal/mol higher than the calculated energy[10] or the energy of the triplet diradical reduced to -35.5 kcal/mol (14.9 kcal/mol lower than the calculated energy), or some combination of these two changes. This new barrier may very well explain the 1 kcal energy content in vinoxy measured by Loison *et al.*,[6] despite the 3 kcal available as translational energy in the incoming $O(^3P)$ from their dissociation at 355 nm. The number we measure is only a lower limit to the intrinsic dissociation lifetime of the diradical, because $1/\tau_{obs} = 1/\tau_{diss} + 1/\tau_{ISC}$, and Schmoltner *et al.* find that an appreciable amount of HCO product comes from the ISC channel. Molecular beam measurements such as theirs are not, however, very accurate measurements of relative product yield.

B. Photodissociation of acetaldehyde

We now turn to the right-hand side of the potential energy surfaces shown in Fig. 1. According to the work of several groups (Refs. 38–42, and references therein), acetal dehyde is statistical limit for internal conversion (IC) from S_1 to S_0 but small molecule for ISC from S_1 to T_1 at its singlet origin (~ 336 nm). From 336 to 317 nm it is still the statistical limit for IC but an intermediate case for ISC.

Above ~317 nm it is the statistical limit for both. The latter identifies the onset of photodissociation which results in one or more of the following products:

$$CH_3CHO \rightarrow CH_3 + HCO \quad (5)$$

$$\rightarrow CH_3CO + H \quad (6)$$

$$\rightarrow CH_4 + CO. \quad (7)$$

The triplet state density apparently rises dramatically just above the reaction threshold and the production of HCO and CH_3CO radicals [channels (5) and (6), respectively] will come exclusively from the triplet pathway.[38–41,43] However, at high energy ($\lambda_{diss} \leqslant 280$ nm) Ohta and Baba suggest that HCO may come from higher vibrational levels of S_1. On the other hand, channel (7) is only correlated to the S_0 of acetaldehyde via the IC from S_1, and the barrier for the production of molecular CO and CH_4 was calculated to be about 85 kcal/mol.[44] This barrier is at the same energy as the vibrationless level of S_1 acetaldehyde.

The energy available in the CH_3+HCO or $H+CH_3CO$ fragments after dissociation at our 266 nm pump is about 18 kcal/mol. This energy should appear as vibrational and rotational quanta in the photofragments. Atkinson and co-workers[45–47] have studied the kinetics following the population of different vibrational and rotational levels of nascent HCO, but their experiment is entirely different from ours. (Their study was conducted in the gas phase using an intracavity laser spectroscopy technique with time resolution in the microsecond scale.) Due to our intrinsically low spectral resolution, we have not attempted to measure the product state distribution.

The transients shown in Fig. 6 for formyl and acetyl radicals suggest the same mechanism for the production of both radicals based on their appearance time ($t=622$ ps for HCO and $t=667$ ps for CH_3CO). We tried to observe similar transients at different pump wavelengths (in the range 280–315 nm), keeping the probe wavelength unchanged, but could not observe any time evolution from either radical within our time delay limit between the pump and the probe pulses of ~2 ns. This observation can be explained by the results of Ohta and Baba.[37] They measured the lifetime of acetaldehyde fluorescence in bulb at different energies and found it to decrease from 5.2 ns at excitation energy near the S_1 origin to 1.0 ns at excitation down to 280 nm, then <0.6 ns at $\lambda_{diss}=275-270$ nm, within their time resolution. In our beam experiment, we did not observe any evolution from either radical in this wavelength range which indicates that acetaldehyde dissociates in a time longer than 2 ns (our maximum scan range) in this region of the spectrum under collisionless conditions. The evolution of the radicals at 266 nm pump energy implies that acetaldehyde *starts* to dissociate in a time shorter than ~100 ps (our pump duration pulse).

Two rates should be considered which control the photodissociation process, the rate of the $T_1 \leftarrow S_1$ ISC and the photodissociation rate from the triplet state to radicals. The rate of the triplet photodissociation following ISC was estimated roughly to be $\sim 10^8$ and $\sim 10^9$ s^{-1} for 315 and 310 nm excitation, respectively.[39] If this rate is the rate determining step, we could have detected the photoproducts at $\lambda_{diss} \leqslant 315$ nm. We have calculated this rate at our pump energy of 266 nm by RRKM theory (for which, unlike the vinoxy case, the energetics are well known) which yields 3.0×10^{12} s^{-1}. This indicates that the rate of photodissociation of acetaldehyde does not contribute to our measured rise times. The radical's appearance rates are then due mainly to the ISC process which increases monotonicly with energy. An exit channel from higher S_1 levels cannot be ruled out at such high energy as suggested by Ohta and Baba[39] and should also be considered. However, the single-exponential rise times observed here indicate that the radical products are due only to one channel.

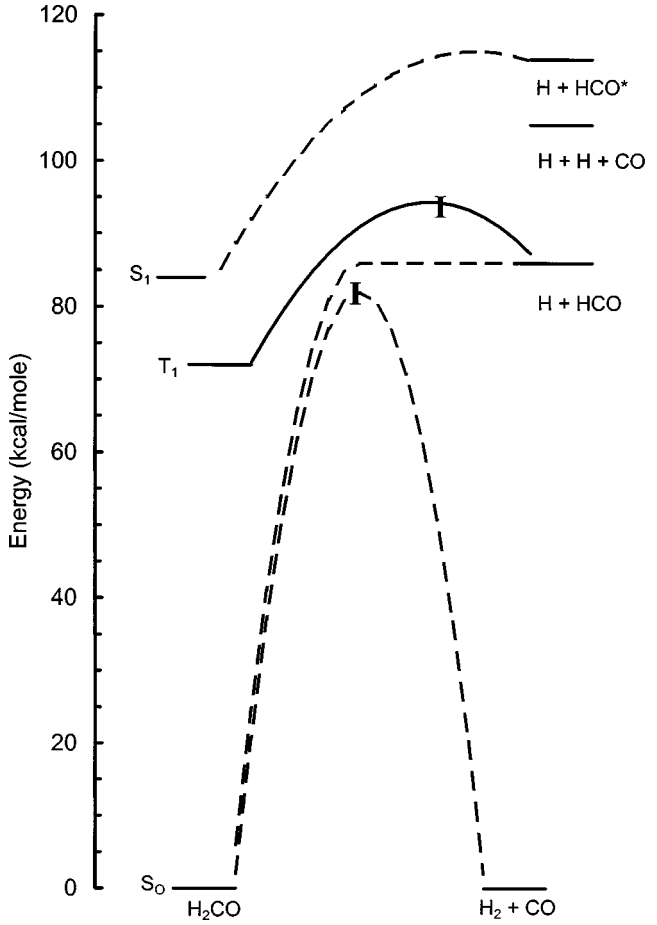

FIG. 9. Energy levels for formaldehyde photodissociation. The solid line representing reaction coordinates represents the triplet, dashed ones represent singlets. (Adapted from Ref. 49.)

The rate of the appearance of HCO from the photodissociation of formaldehyde at the same λ_{diss} of 266 nm is faster than that from acetaldehyde. We have measured this rate to be 390 ps (Fig. 7). The onset of photodissociation of HCHO to H+HCO has been measured to be around 330 nm.[48,49] The energy surfaces representing the photodissociation processes of formaldehyde are shown in Fig. 9 (adopted from the work of Moore[49]). The quantum yield of the HCO radical increases as λ decreases. According to Fig. 9, HCO can be produced without a barrier from S_0 formaldehyde. As the dissociation energy increases, the rate of $T_1 \leftarrow S_1$ ISC increases and a barrier to dissociation occurs from T_1 at

about 311 nm for HCO production. This situation resembles the production of HCO from the triplet acetaldehyde. The rate of ISC in formaldehyde was measured to be $4 \times 10^7\ s^{-1}$ near the barrier.[49] This rate, as in the case of acetaldehyde, gets faster as the energy increases over the barrier. The photodissociation rate must be greater than the $3 \times 10^{12}\ s^{-1}$ of acetaldehyde photodissociation. The observed single-exponential rise time of HCO also indicates that we detect only one exit channel at such high energy which is most likely the triplet photodissociation.

We now return to the observation of acetyl radical by REMPI. Little is known about the spectroscopy of CH_3CO.[50–52] The lack of structure in its absorption spectrum suggests that it strongly predissociates in the UV visible spectral region into CH_3+CO.[50] All indications are that its electronic structure is exactly what would be expected by analogy to HCO.

The measured rate of appearance of CH_3CO in Fig. 6 is similar to that measured for HCO at the same probe energy of 400 nm. This means that a similar mechanism is involved in the production of both radicals from the photodissociation of acetaldehyde and a similar mechanism for the production of both ions by REMPI.

The question now is, which REMPI mechanism the acetyl radical follows to ionization. We propose the REMPI $(2+1)$ mechanism based on the following observation. We performed a power-dependent experiment by measuring the ion intensity as a function of the probe power. This experiment did not lead to any conclusive result, but in all cases the ion intensity ratio CH_3CO^+/HCO^+ remains the same (~ 2). We know from the work of Tjossem *et al.*[21] that the REMPI mechanism for the production of HCO^+ is $(2+1)$. Accordingly, the same mechanism can be proposed for CH_3CO^+. Also, the ionization potential of CH_3CO is 6.84 eV.[53] The probe energy at 400 nm is well above this threshold if we consider a $(2+1)$ mechanism.

V. CONCLUSION

The reaction between $O(^3P)$ and C_2H_4 has been studied in a restricted geometry under cold-isolated conditions using a pump–probe technique with LIF detection. The decomposition lifetime of the intermediate triplet diradical was measured to be 217 ps. This intermediate (CH_2CH_2O) is formed immediately after the oxygen atom attacks one carbon atom of the ethylene molecule. This step is followed by fragmentation to hydrogen and vinoxy through a late high barrier. The geometry of the precursor complex $C_2H_4 \cdot NO_2$ has been calculated using the sum of 6–12 atom–atom potentials. The calculated geometry fits the model described for similar van der Waals molecules.

The unimolecular side of the potential energy surfaces of the above reaction has been investigated by studying the photodissociation of acetaldehyde. Fragments from this photodissociation were detected by REMPI-TOFMS. The real time evolution of HCO and CH_3CO photofragments were measured and found to be close within the experimental errors. The results imply a similar mechanism of dissociation. The ISC rate from S_1 to T_1 is found to be the rate determining step. At about 7.5 kcal/mol of translational energy, the evolution of HCO and CH_3CO could be observed with rise times of 622 and 667 ps, respectively. A $(2+1)$ REMPI mechanism is suggested for the production of CH_3CO^+ by comparing the results of both CH_3CO^+ and HCO^+.

The evolution of HCO from the photodissociation of formaldehyde is measured to be shorter than the evolution of HCO from acetaldehyde by about 200 ps indicating a faster $T_1 \leftarrow S_1$ ISC rate in the former.

ACKNOWLEDGMENT

This material is based upon work supported by the National Science Foundation under Award No. CHE-95-28835.

[1] R. J. Cvetanovic and D. L. Singleton, Rev. Chem. Intermediates **5**, 183 (1984).
[2] W. C. Brider, in *Combustion Chemistry* (Springer, New York, 1984).
[3] B. J. Finlayson-Pitts and J. N. Pitts, Jr., *Atmospheric Chemistry: Fundamentals and Experimental Techniques* (Wiley, New York, 1986).
[4] A. M. Schmoltner, P. M. Chu, R. J. Brudzynski, and Y. T. Lee, J. Chem. Phys. **91**, 6926 (1989).
[5] J. Kleinermanns and A. C. Luntz, J. Phys. Chem. **85**, 1966 (1981).
[6] J. C. Loison, C. Dedonder-Lardeux, C. Jouvet, and D. Solgadi, J. Phys. Chem. **95**, 9192 (1991).
[7] J. C. Loison, C. Dedonder-Lardeux, C. Jouvet, and D. Solgadi, Ber. Bunsenges. Phys. Chem. **96**, 1142 (1992).
[8] J. C. Loison, C. Dedonder-Lardeux, C. Jouvet, and D. Solgadi, Faraday Discuss. **97**, 379 (1994).
[9] M. G. Moss, J. W. Hudgens, and J. D. McDonald, J. Chem. Phys. **72**, 3486 (1980).
[10] T. Fueno, Y. Takahara, and K. Yamaguchi, Chem. Phys. Lett. **167**, 291 (1990).
[11] B. J. Smith, M. Tho Nguyen, W. J. Bouma, and L. Radom, J. Am. Chem. Soc. **113**, 6452 (1991).
[12] H. Zacharias, M. Geilhaupt, K. Meier, and K. H. Welge, J. Chem. Phys. **74**, 218 (1981).
[13] S. I. Ionov, G. A. Brucker, C. Jaques, Y. Chen, and C. Wittig, J. Chem. Phys. **99**, 3420 (1993).
[14] S. A. Wright, M. F. Tuchler, and J. D. McDonald, Chem. Phys. Lett. **226**, 570 (1994).
[15] M. F. Tuchler, S. A. Wright, and J. D. McDonald, J. Chem. Phys. **106**, 2634 (1997).
[16] S. A. Wright and J. D. McDonald, Rev. Sci. Instrum. **65**, 265 (1994).
[17] G. Inoue, Y. Nakata, Y. Usui, H. Akimoto, and M. Okuda, J. Chem. Phys. **70**, 3689 (1979).
[18] L. R. Brock and E. A. Rohlfing, J. Chem. Phys. **106**, 10 048 (1997).
[19] G. Inou and H. Akimoto, J. Chem. Phys. **74**, 425 (1981).
[20] J. A. Booze and T. Baer, J. Chem. Phys. **96**, 5541 (1992).
[21] P. J. H. Tjossem, P. M. Goodwin, and T. A. Cool, J. Chem. Phys. **84**, 5334 (1986).
[22] G. J. Fisanick and T. S. Eichelberger, IV, J. Chem. Phys. **74**, 6692 (1981).
[23] S. K. Shin, B. Kim, J. G. Haldeman, and S.-J. Han, J. Phys. Chem. **100**, 8280 (1996).
[24] A. M. Andrews, A. Taleb-Bendiab, M. S. Labarge, K. W. Hillig II, and R. L. Kuczkowski, J. Chem. Phys. **93**, 7030 (1990).
[25] C. W. Gillies, J. Z. Gillies, R. D. Suenram, F. J. Lovas, E. Krata, and D. Cremer, J. Am. Chem. Soc. **113**, 2412 (1991).
[26] G. Nemethy, M. S. Pottle, and H. A. Scheraga, J. Phys. Chem. **87**, 11 (1983).
[27] M. D. Harmony, V. W. Laurie, R. L. Kuczkowski, R. H. Schwendeman, D. A. Ramsay, F. J. Lovas, W. J. Lafferty, and A. G. Maki, J. Phys. Chem. Ref. Data **8**, 619 (1979).
[28] D. C. Robie, M. Hunter, J. L. Bates, and H. Reisler, Chem. Phys. Lett. **193**, 413 (1992).
[29] S. I. Ionov, G. A. Brucker, C. Jaques, L. Valachovic, and C. Wittig, J. Chem. Phys. **97**, 9486 (1992).
[30] J. Segall, Y. Wen, C. Wittig, A. Garcia-Vela, and R. B. Gerber, Chem. Phys. Lett. **207**, 504 (1993).
[31] D. S. King, D. G. Sauder, and M. P. Casassa, J. Chem. Phys. **100**, 4200 (1994).
[32] R. J. Cvetanovic, J. Chem. Phys. **23**, 1375 (1955).
[33] R. J. Cvetanovic, Adv. Photochem. **1**, 155 (1963).

[34] R. J. Buss, R. J. Baseman, G. He, and Y. T. Lee, J. Photochem. **17**, 389 (1981).
[35] J. McFarlane, J. C. Polanyi, and J. G. Shapter, J. Photochem. Photobiol., A **58**, 139 (1991).
[36] J. D. McDonald, Ph.D. thesis, Harvard University, 1971.
[37] M. Dupuis, J. J. Wendoloski, T. Takada, and W. A. Lester, Jr., J. Chem. Phys. **76**, 481 (1982).
[38] R. J. Gill and G. H. Atkinson, Chem. Phys. Lett. **64**, 426 (1979).
[39] H. Ohta and H. Baba, J. Phys. Chem. **90**, 2654 (1986).
[40] T. Kono, M. Takayanagi, T. Nishiya, and I. Hanazaki, Chem. Phys. Lett. **201**, 166 (1993).
[41] T. Gejo, H. Bitto, and J. R. Huber, Chem. Phys. Lett. **261**, 443 (1996).
[42] S.-H. Lee and I.-C. Chen, Chem. Phys. **220**, 175 (1997).
[43] N. Ohta, T. Koguchi, T. Takemura, and I. Suzuka, Chem. Phys. Lett. **191**, 232 (1992).
[44] J. S. Yadav and J. D. Goddard, J. Chem. Phys. **84**, 2682 (1986).
[45] R. J. Gill, W. D. Johnson, and G. H. Atkinson, Chem. Phys. **58**, 29 (1981).
[46] F. Stoeckel, M. D. Schuh, N. Goldstein, and G. H. Atkinson, Chem. Phys. **95**, 135 (1985).
[47] N. Goldstein and G. H. Atkinson, Chem. Phys. **105**, 267 (1986).
[48] A. C. Terenties and S. H. Kable, Chem. Phys. Lett. **258**, 626 (1996).
[49] M.-C. Chuang, M. F. Foltz, and C. B. Moore, J. Chem. Phys. **87**, 3855 (1987).
[50] M. E. Jacox, Chem. Phys. **69**, 407 (1982).
[51] H. Li, Q. Li, W. Mao, Q. Zhu, and F. Kong, J. Chem. Phys. **106**, 5943 (1997).
[52] N. C. Baird and H. B. Kathpal, Can. J. Chem. **55**, 863 (1977).
[53] E. Murad and M. G. Inghram, J. Chem. Phys. **40**, 3263 (1964).